Journal of Applied Sciences

ISSN 1812-5654

science alert

ANSInet
an open access publisher
http://ansinet.com

Journal of Applied Sciences 11 (8): 1391-1395, 2011
ISSN 1812-5654 / DOI: 10.3923/jas.2011.1391.1395

Synthesis and Characterization of Silica-supported Iron Nanocatalyst by Modified Colloidal Method

[1]Nor Aziyan Mohd Nasir, [2]Noor Asmawati Mohd Zabidi and [2]Chong Fai Kait
[1]Department of Chemical Engineering,
[2]Department of Fundamental and Applied Sciences,
Universiti Teknologi PETRONAS, Bandar Seri Iskandar, Tronoh 31750, Perak, Malaysia

Abstract: Silica-supported iron nanocatalysts for Fischer-Tropsch Synthesis (FTS) were prepared using the modified colloidal method in the presence of surfactants in an organic medium. The iron loading on silica support was varied at 3, 5 and 6 wt.%. The samples were characterized by XPS, TPR and TEM. The presence of Fe_2O_3 on the silica support was confirmed by XPS. TPR analysis showed that the increase in Fe loading caused the first reduction temperature of the nanocatalysts to shift to a higher temperature. TEM analysis revealed that the iron nanoparticles were not uniformly distributed on the silica support. The size of iron nanoparticles ranged from 4 to 20 nm. For the 3 and 5 wt.% Fe/SiO_2, the size of the iron nanoparticles were mostly in the range of 1-5 nm, whereas for the 6 wt%, most of the iron nanoparticles (74%) were in the range of 6-10 nm.

Key words: Silica support, iron nanocatalyst, XPS, TPR, TEM

INTRODUCTION

Fischer-Tropsch Synthesis (FTS) has been recognized as an important technology in the production of liquid fuels and chemicals from syngas derived from coal, natural gas, and other carbon-containing materials (Zhao *et al*., 2008). The main aim of FTS research is to improve the selectivity for C_{5+} hydrocarbons and to decrease the selectivity for methane, and the key to realizing this aim is to develop FT catalyst with high activity and selectivity (Lihong *et al*., 2007).

Although several metals (including Co, Ni, and Ru) have been considered as the most commonly active component for FTS catalysts, iron-based catalysts are widely used because of the high FTS activity, low cost, flexible product distribution and favorable engineering characteristics (Ding *et al*., 2008). The properties of iron nanoparticles depend on its size; smaller particles should improve the kinetics of the reactions (Huber, 2005).

In this study, iron nanocatalyst was prepared by the modified colloidal method. The modified colloidal method is the preferred catalyst preparation method because it can result in nanocatalyst particle having size 4 to 15 nm, which is expected to have high activity and selectivity for FTS (Zabidi, 2007). Colloidal synthesis has been widely used as an efficient route to control metal particle size and shape, crystallinity and crystal structure (Khodakov *et al*., 2007). Colloids are synthesized in the presence of surfactants which disperse and stabilize the nanoparticles in an organic solvent. Some of the approaches include polyol method, ethylene glycol method, modified coordination capture method and pseudo-colloidal method. The polyol process involves heating a mixture of catalyst precursor in surfactants, such as oleic acid and oleyl amine in high-boiling solvent such as diphenyl ether (Zabidi, 2007). The size of the nanoparticles is controlled by changing the concentration of the precursor, the amount and type of surfactant, the aging time and temperature of the reaction.

High temperature alcohol reduction of iron(III) acetylacetonate metal precursor resulted in monodisperse iron nanoparticles. This synthesis process is also called "heating-up" process (Khodakov *et al*., 2007). Another synthetic method that produces uniform nanocrystals that is comparable to the "heating-up" process is called the "hot injection" method. The "hot injection" method induces high supersaturation and leads to fast homogeneous nucleation reaction followed by diffusion-controlled growth process, which control the particle size distribution.

The objective of this research was to prepare a spherical model nanocatalyst comprising iron nanoparticles supported on silica spheres. This report will highlight the effect of iron loading on the properties of the

Corresponding Author: Noor Asmawati Mohd Zabidi, Department of Fundamental and Applied Sciences, Universiti Teknologi PETRONAS, Bandar Seri Iskandar, Tronoh 31750, Perak, Malaysia

nanocatalysts. Powdered samples were characterized using X-ray Photoelectron Spectroscopy (XPS), Temperature Programmed Reduction (TPR) and Transmission Electron Microscopy (TEM).

MATERIALS AND METHODS

Synthesis of iron nanocatalyst: The iron nanocatalyst was prepared by the modified colloidal method (Zabidi, 2007). The experimental setup used in synthesizing the SiO_2-supported iron nanocatalyst is shown in Fig. 1. Silica (SiO_2) spheres (BET surface area: 23.6 m^2g^{-1}, pore volume: 0.14 m^3g^{-1}) were synthesized using the Stöber method. The SiO_2 spheres were added to a surfactant mixture (designated as mixture A) containing oleic acid, oleylamine, cyclohexane and then placed in a bath sonicator for 3 h. Mixture A was poured into the multi-neck reaction vessel and heated to 265°C using a digital heater controller (Thermo Fischer Scientific EM 0100/CE) under nitrogen flow. The slurry was stirred at 200 rpm using a mechanical stirrer (Heidolph RZR 2021) throughout the synthesis period.

Another mixture (designated as mixture B) was prepared by mixing Fe $(acac)_3$, 1, 2 hexanedecanediol, oleic acid, oleylamine, and phenyl ether. The amount of $Fe(acac)_3$ was varied according to the desired iron loading (3, 5 and 6 wt.%). The molar ratio of Fe $(acac)_3$ to surfactant was kept at 1:18. Mixture B was placed in the bath sonicator for about 20 min to prevent crystallization of the phenyl ether solvent.

Mixture B was added dropwise to mixture A once the temperature of mixture A reached 150°C. The resultant black mixture was heated until the temperature reached 265°C. When the temperature reached 265°C, the mixture was heated for another hour. Then, the black mixture was cooled under nitrogen flow until the temperature decreased to 90°C. Ethanol was then added to the cooled reaction mixture to precipitate the nanoparticles. The solid was separated by centrifugation at 7000 rpm for 90 min. The precipitates obtained after the centrifugation was calcined in air at 450°C for 2 h in a furnace.

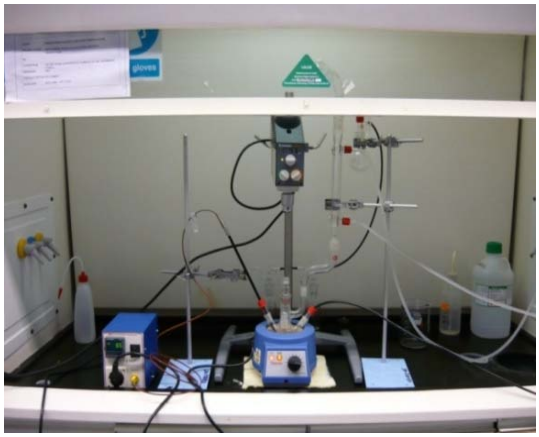

Fig. 1: Experimental setup

Characterization technique

XPS analysis: Surface analysis was conducted using XPS (Thermo Scientific K alpha) equipped with monochomatized Al Kα X-ray source and chaneltron detector. Analysis was carried out at vacuum $<10^{-9}$ Torr. Powdered samples were placed in the holes of the sample holder block and scanned at pass energy of 50.0 eV.

TPR analysis: TPR analysis was conducted using TPD/R/O 1100 (Thermo Electron) to determine the reduction profile of the catalysts. A flow of 5%H_2/95%N_2, maintained at 50 cc min^{-1} was used as the reducing gas. Typically, 0.1 g samples were reduced using 5%H_2/95%N_2 and heated to 800°C at a rate of 5°C min^{-1}.

TEM analysis: TEM analysis was conducted to observe the distribution of iron nanoparticles on the SiO_2 support. TEM images were obtained using Philip Tecnai 20 with accelerating voltage of 200 kV.

RESULTS AND DISCUSSION

XPS analysis: Figure 2 shows the XPS spectra of the Fe 2p region for the 3 and 5 wt.% Fe/SiO_2 nanocatalysts. The binding energies of the Fe 2p peaks are shown in Table 1.

The XPS results show that the Fe $2p_{3/2}$ peak was more intense than that of the Fe $2p_{1/2}$ peak. This is because of the spin orbit (j-j) coupling; Fe $2p_{3/2}$ has degeneracy of

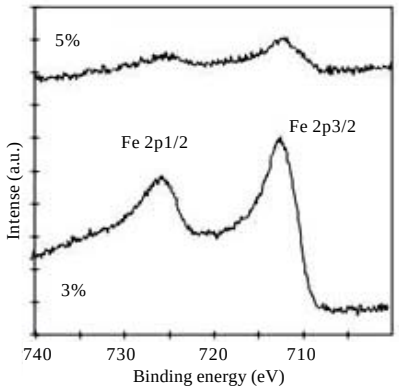

Fig. 2: XPS spectra of Fe 2p region for the 3 and 5% Fe/SiO_2

Table 1: Binding energies for Fe 2p peaks

	Binding energy (eV)	
Samples	Fe $2p_{1/2}$	Fe $2p_{3/2}$
3 wt.% Fe/SiO_2	725.1	711.8
5 wt.% Fe/SiO_2	725.3	712.5
Fe_3O_4[1]	724.1	710.6
Fe_2O_3[1]	724.6	711.0

[1]Yamashita and Hayes (2008)

Table 2: Binding energy of O 1s for Fe/SiO_2 nanocatalyst

Samples	Binding energy (eV) for O 1s
3 wt.% Fe/SiO_2	533.0
5 wt.% Fe/SiO_2	533.1
Fe_2O_3[1]	527.0
Fe_3O_4[1]	531.0
SiO_2[2]	531.5

[1]Yamashita and Hayes (2008), [2]Mekki (2005)

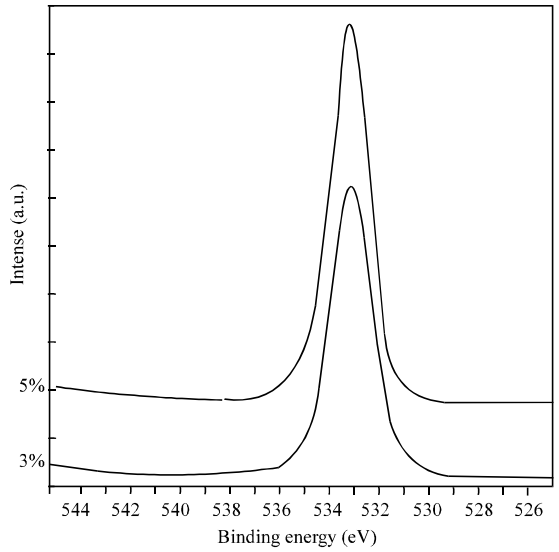

Fig. 3: XPS spectra of O 1 s for 3 and 5 wt.% Fe/SiO_2 nanocatalyst

four states whilst Fe $2p_{1/2}$ has only two states (Yamashita and Hayes, 2008). The peak positions of Fe $2p_{3/2}$ and Fe $2p_{1/2}$ for the Fe_3O_4 are 710.6 (SD = 0.05) and 724.1 eV (SD = 0.07), respectively (Yamashita and Hayes, 2008). For Fe_2O_3, the binding energies reported in the literature are 711.0 (SD. = 0.01) and 724.6 (SD = 0.17) for Fe $2p_{3/2}$ and Fe $2p_{1/2}$, respectively (Yamashita and Hayes, 2008). The peak positions of Fe $2p_{3/2}$ and Fe $2p_{1/2}$ obtained for the Fe/SiO_2 samples were in the range of Fe_2O_3 peaks reported in the literature. The 0.8 ev shift between the experimental binding energy of Fe $2p_{3/2}$ and that of the literature value could be due to the metal–support interaction since the binding energy reported in the literature is for the unsupported Fe_2O_3.

Figure 3 shows the XPS spectra of O1s for Fe/SiO_2 nanocatalysts and the binding energies are shown in Table 2.

Table 3: Reduction temperatures of Fe/SiO_2 nanocatalysts

	Reduction temperature (°C)		
Wt.%	$Fe_2O_3 \rightarrow Fe_3O_4$	$Fe_3O_4 \rightarrow FeO$	$FeO \rightarrow Fe$
3	373	Not detected	610
5	378	457	595
6	379	422	638
Literature[1]	241-389	332-443	663-697

[1]Yu *et al.* (2008)

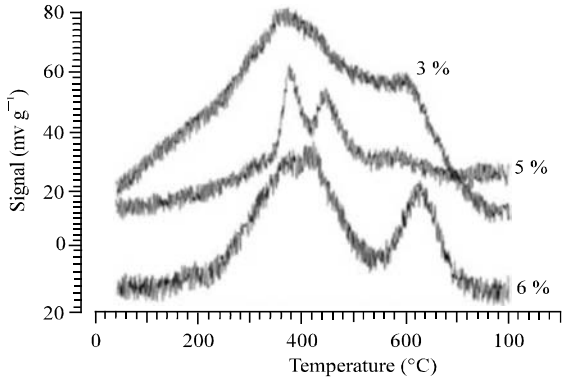

Fig. 4: TPR profiles for 3, 5 and 6% Fe/SiO_2

As shown in Table 2, the binding energy of O 1s for both Fe/SiO_2 samples was 533 eV. The O 1s peak was contributed by both iron oxide and the silica support (SiO_2). From literature, the O1s binding energy value for Fe_3O_4 is 531 eV while that of Fe_2O_3 is 527 eV (Yamashita and Hayes, 2008). Meanwhile, the binding energy value for O 1s of SiO_2 is 531.5 eV (Mekki, 2005). The shift in binding energy for O1s peak between the SiO_2-supported Fe catalyst and that of Fe_2O_3 could be due to the strong Fe-SiO_2 interaction.

TPR analysis: Figure 4 and Table 3 show the results of TPR analysis for 3, 5, and 6 wt.% Fe/SiO_2 nanocatalysts.

As shown in Fig. 4, the TPR profiles of the three nanocatalysts show two distinct reduction stages in the temperature range of 370-640°C. The first reduction stage, containing two partially overlapped peaks, can be assigned to the transformations of $Fe_2O_3 \rightarrow Fe_3O_4$ and $Fe_3O_4 \rightarrow FeO$ (Yu *et al.*, 2008). The second reduction stage can be assigned to the transformation of $FeO \rightarrow Fe$, which is the reduction of Fe_3O_4 to α-Fe via wüstite (FeO) as an intermediate (Yu *et al.*, 2008). The TPR results were in agreement with the XPS results, which confirmed the presence of Fe_2O_3.

As shown in Table 3, the increase in Fe loadings caused the first reduction temperature of the nanocatalysts to shift to higher temperature. However, increase of Fe loadings did not strongly influence the reduction of $Fe_3O_4 \rightarrow FeO$ and $FeO \rightarrow Fe$ as the thermodynamics of the process involved the nucleation of new crystal structures instead of H_2 dissociation steps that control the reduction rates at higher temperatures (Pour *et al.*, 2008).

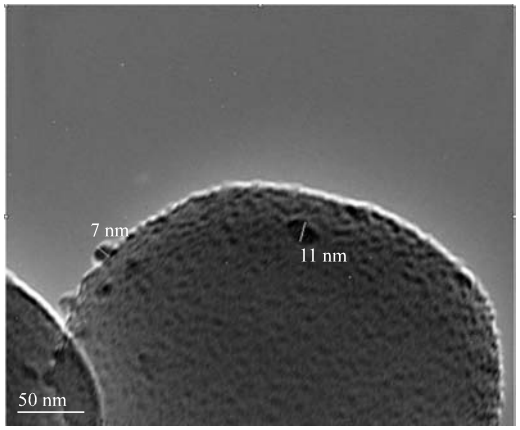

Fig. 5: TEM image of 3% Fe/SiO_2

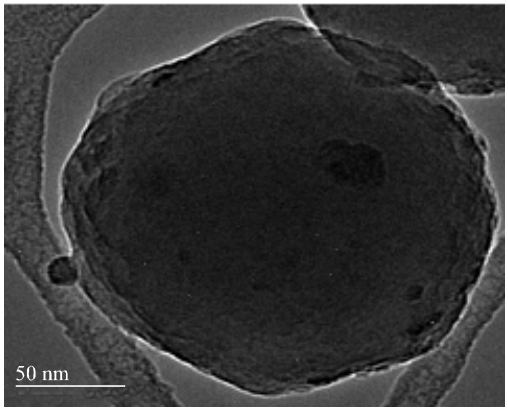

Fig. 6: TEM image of 5% Fe/SiO_2

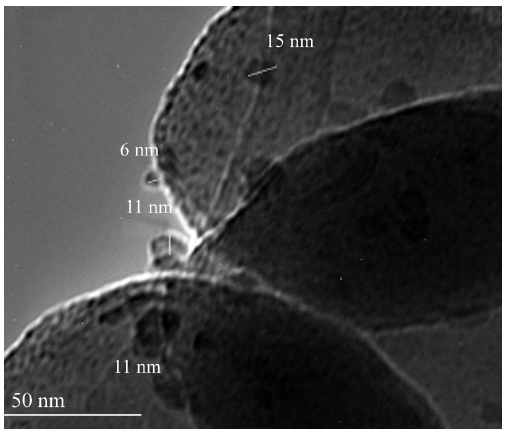

Fig. 7: TEM image of 6% Fe/SiO_2

TEM analysis: Figure 5, 6 and 7 show the TEM images for 3, 5 and 6 wt. % Fe/SiO_2 nanocatalyst, respectively.

Profile views of the iron nanoparticles supported on SiO_2 spheres were obtained using TEM. However, some of the surface of SiO_2 support remain bare, indicating uneven deposition of iron nanoparticles on the support. Figure 8 shows the histogram of the size distribution of iron nanoparticles on silica support for the three samples prepared in this study.

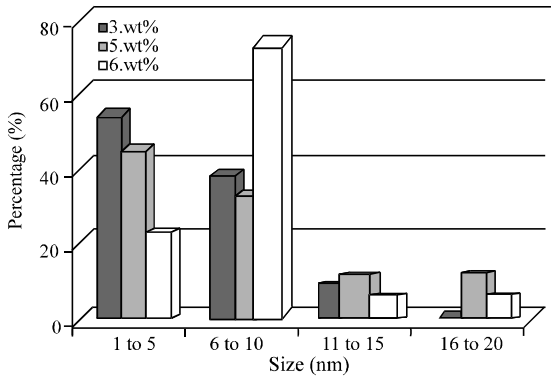

Fig. 8: Size distribution of iron nanoparticles for 3, 5 and 6 wt.% $FeSiO_2$

The size of the iron nanoparticles for the 3 and 5 wt.% Fe/SiO_2 were mostly in the range of 1-5 nm (54% for 3 wt. % Fe/SiO_2 and 45% for 5 wt.% Fe/SiO_2), meanwhile for the 6 wt.% Fe/SiO_2 the size of the iron particles were mostly in the range of 6-10 nm (74%). The 6.wt% Fe/SiO_2 had a narrower particle size distribution compared to those of 3 and 5 wt.% Fe/SiO_2 samples. The target iron particle size is between 4-10 nm. Therefore, it can be concluded that the size of iron nanoparticles obtained from all the three catalysts synthesized in this work were in the target range. The 6.wt % Fe/SiO_2 nanocatalyst was the best catalyst model amongst the three samples investigated in this work because it showed a better particle size distribution compared to the other two samples.

CONCLUSION

Silica supported iron nanocatalyst have been synthesized by the modified colloidal method. The nanoparticles were synthesized at iron loadings of 3, 5 and 6.wt % while the ratio between the precursor and the surfactant was maintained at 1:18. XPS analysis revealed the presence of Fe_2O_3 on the SiO_2 support. TPR analysis showed that the increase of Fe loadings caused the first reduction temperature of the nanocatalysts to shift to higher temperature. TEM analysis enabled profile views of the SiO_2-supported Fe nanocatalyst to be captured. The size of iron particles were in the range of 4 to 20 nm. The 6.wt % Fe/ SiO_2 showed a narrower particle size distribution than those obtained from the other two

catalyst models and was chosen as the best spherical catalyst model.

ACKNOWLEDGMENT

The authors acknowledge financial support provided by MOSTI E-Science Fund (Project No. 03-02-02-SF0036).

REFERENCES

Ding, M., Y. Yang, J. Xu, Z. Tao, H. Wang, H. Wang, H. Xiang and Y. Li, 2008. Effect of reduction pressure on precipitated potassium promoted iron-manganese catalyst for Fischer-Tropsch synthesis. Applied Catalysis A., 345: 176-184.

Huber, D.L., 2005. Synthesis, properties and applications of iron nanoparticles. Small, 5: 482-501.

Khodakov, A.Y., W. Chu and P. Fongarland, 2007. Advances in the development of novel cobalt fischer-tropsch catalysts for synthesis of long-chain hydrocarbons and clean fuels. Chem. Rev., 5: 1692-1744.

Lihong, S., L. Debao, H. Bo and S. Yuhan, 2007. Organic modification of SiO_2 and its influence on the properties of co-based catalysts for fischer-tropsh synthesis. Chinese J. Catalysis, 28: 999-1002.

Mekki, A., 2005. X-ray photoelectron spectroscopy of $Ce)_2$-Na_2O-SiO_2 glasses. J. Electron Spectroscopy Related Phenomena, 142: 75-81.

Pour, A.N., S.M.K. Shahri, H.R. Bozorgzadeh, Y. Zamani, A. Tavasoli and M.A. Marvast, 2008. Effect of Mg, La and Ca promoters on the structure and catalytic behavior of iron-based catalysts in Fischer-Tropsch synthesis. Applied Catalysis A., 348: 201-208.

Yamashita, T. and P. Hayes, 2008. Analysis of XPS spectra of Fe^{2+} and Fe^{3+} ions in oxide materials. Applied Surface Sci., 254: 2441-2449.

Yu, W., B. Wu, J. Xu, Z. Tao, H. Xiang and Y. Li, 2008. Effect of Pt impregnation on a precipitated iron-based fischer-tropsch synthesis catalyst. Catalysis Lett., 125: 116-122.

Zabidi, N.A.M.M., 2007. Sabbatical Report. Eindhoven University of Technology, The Netherlands.

Zhao, G., C. Zhang, S. Qin, H. Xiang and Y. Li, 2008. Effect of interaction between potassium and structural promoters on Fischer-Tropsch performance in iron-based catalysts. J. Mol. Catalysis A., 286: 137-142.